Journal of Applied Polymer Science

Linear-Nonlinear Dichotomy of the Rheological Response of Particle-Filled Polymers

Amy M. Randall,* Christopher G. Robertson†
Bridgestone Americas, Center for Research and Technology, Akron, Ohio 44301
*Present address: Bridgestone Americas Tire Operations, 10 East Firestone Blvd., Akron OH 44317;
E-mail: randallamy@bfusa.com.
†Present address: Eastman Chemical Company, Rubber Additives, 260 Springside Dr., Akron OH 44333;
E-mail: crobertson@eastman.com.
Correspondence to: C. G. Robertson (E-mail: crobertson@eastman.com)

ABSTRACT: Novel nanoparticles, polymer-particle coupling agents, and functionalized polymers are being developed to enhance the performance of particle-reinforced polymer systems such as advanced rubber compounds for automobile tires. Understanding the complex rheological behavior of rubber is critical to providing insights into both processability and end-use properties. One unique aspect of the rheology of filled elastomers is that the incorporation of particles introduces a hysteretic softening (Payne effect) at small dynamic strains. This study demonstrates that this nonlinear viscoelastic behavior needs to be considered when attempting to correlate steady shear response (Mooney viscosity) to oscillatory shear measurements from test equipment such as the Rubber Process Analyzer (RPA). While a wide array of unfilled gum elastomers show good correlation between Mooney viscosity and dynamic torque from the RPA at all of the strain amplitudes used, rubber compounds containing silica and carbon black particles only exhibit good agreement between the two measures of processability when the oscillatory strain amplitude is high enough to sufficiently break up the filler network. Other features of the filler network and its influence on nonlinear rheology are considered in this investigation, including the effects of polymer–filler interactions on filler flocculation and the use of Fourier transform rheometry to illustrate the "linear-nonlinear dichotomy" of the Payne effect. © 2014 Wiley Periodicals, Inc. J. Appl. Polym. Sci. **2014**, *131*, 40818.

KEYWORDS: elastomers; nanoparticles; rheology; rubber; viscosity and viscoelasticity

Received 16 December 2013; accepted 27 March 2014
DOI: 10.1002/app.40818

INTRODUCTION

The need to comprehend the complex rheological behavior of rubber is ever-present as the rubber industry continually innovates to incorporate new technology into products. Functionalized polymers, non-traditional nanoparticles, polymer–particle coupling agents, reactive mixing, and other new technologies are being utilized in tires and other rubber applications. The rheology of uncured compounds affects the processability of the rubber, and the viscoelasticity of the cured rubber influences the performance of the material in the final application. The viscoelastic properties of rubber used in tire treads, for example, have direct impact on the traction, handling/cornering characteristics, and rolling resistance of automobile tires.

Even though the flow behavior of rubber is quite complex, the most reported and widely recognized measurements of processability and viscosity of rubber are from a simple test using the steady shear Mooney viscometer (ASTM D1646).[1] The Mooney viscometer was invented by Dr. Melvin Mooney in the 1930s, and it remains a standard in the rubber industry today despite the limitations of this simplistic testing approach. Therefore, it is not surprising that data correlations are made with respect to Mooney viscometer results as new rheometer technologies are developed, such as the Rubber Process Analyzer (RPA) which operates in oscillatory shear mode. Dick and Pawlowski[2,3] found that the complex dynamic viscosity η^* (or complex torque S^*) at 7% strain, 0.1 Hz, and 100°C from the RPA correlated well with the Mooney viscosity values (ML_{1+4}) at 100°C for a wide variety of unfilled gum polymers. While this relationship was verified for unfilled elastomers in this prior study, such a correlation between steady shear viscosity and small-strain dynamic properties is not anticipated for particle-filled elastomers due to the additional viscoelastic complexities that arise when particles are present in the rubber.

The particles that are used to reinforce rubber can greatly complicate the viscoelastic response; hence, there is an ongoing

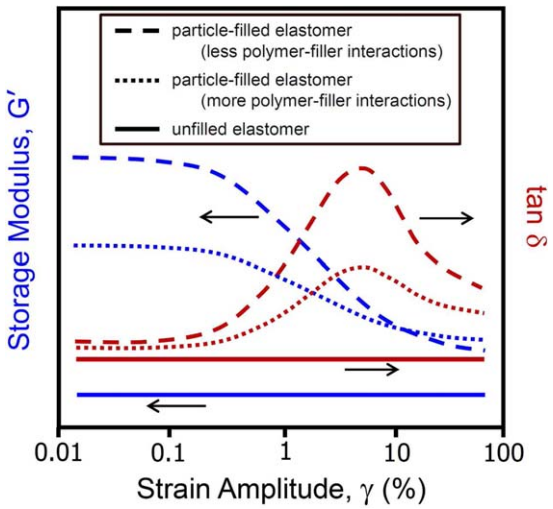

Figure 1. General graphic representation of the Payne effect. Technologies such as end-functionalized polymers and polymer-filler coupling agents (e.g., silanes for silica-reinforced rubber) reduce the magnitude of the Payne Effect by increasing the polymer–filler interactions. [Color figure can be viewed in the online issue, which is available at wileyonlinelibrary.com.]

desire to develop a better understanding of the rheology of nanoparticle-filled elastomers. The addition of nanometer-sized filler particles, such as precipitated silica and carbon black, results in enhancements in numerous physical properties of rubber compounds.[4] One potential disadvantage of filler incorporation in rubber, however, is that the particles can form filler networks within the polymer which undergo hysteretic break-up at small strains (Payne effect).[5–9] Whereas unfilled elastomers typically exhibit strain-dependent (nonlinear) dynamic mechanical properties only at relatively high strains (>100%), the same materials that contain particles at sufficient loading can show this Payne effect which is characterized by striking strain-dependences of dynamic storage modulus (G') and loss modulus (G'') at very low oscillatory strain amplitudes (e.g., in the range from 0.1% to 10%). A general depiction of the Payne effect is provided in Figure 1, including the usual influence of polymer-filler interactions (or reactions) on the behavior.

One unusual aspect of the Payne effect compared to other types of viscoelastic nonlinearity is that the response to forced oscillation is sinusoidal and essentially absent of higher order harmonics at all of the strain amplitudes considered even though the dynamic moduli are so strongly influenced by the strain amplitude.[10] This has been called the "linear-nonlinear dichotomy" of the Payne effect[11] and has also been referred to as the "harmonic paradox".[12] The term "linear-nonlinear dichotomy" captures the observation that the viscoelastic behavior is nonlinear in the sense that the storage and loss modulus depend strongly on the strain amplitude while, in contrast, linearity is implied at each of the strain amplitudes based on the sinusoidal stress response which is simply offset from the oscillatory strain input (or vice versa for stress-controlled rheometers).

When filled rubber compounds are used in tires, the Payne effect hysteresis has an undesirable effect on the fuel economy by increasing the tire rolling resistance. The rolling resistance of tires can consume from 5% to 15% of the fuel energy for passenger cars and 15% to 30% for heavy trucks.[13] The viscoelastic energy losses of the rubber compounds in the tire, especially the tread, greatly impact the rolling resistance.[14] The hysteretic break-up and reformation of the filler network (Payne effect) during tire deformation is a major contributor to these losses.[10] This is why modifying the polymer-filler interface, for example by using silanes in silica-filled tread formulations or using functionalized polymers, as well as dispersing the filler particles are of critical importance in current tire tread technologies. It was noted that the majority of the filler network develops when the mixed rubber is annealed at elevated temperatures, such as during the initial portion of the cure process when the polymer is not yet fully crosslinked. This is often called filler flocculation, and this phenomenon is well documented in particle-reinforced elastomer compounds.[15–22] Known technological approaches for suppressing the filler flocculation process include introducing various silanes in silica-filled rubber[15,17,21] or using modified polymers which have functional groups designed for surface reaction/interaction with carbon black, silica, or other nanoparticles.[23–25]

The commercial importance of particle–elastomer composites and the rich physics involved with the viscoelastic behavior of these materials are motivations for this present study. Given the contribution of the Payne effect, the role of strain amplitude on the ability to relate dynamic properties from the RPA to Mooney viscosity is examined for a wide variety of filled rubber compounds. The impact of polymer-filler interactions on filler flocculation and on the related strain-dependence of dynamic mechanical response is shown by the use of end-functionalized polymers. Fourier transform rheometry[26–29] and Lissajous plots[30] are also applied to further investigate the linear–nonlinear dichotomy of the Payne effect.

EXPERIMENTAL

Test Materials

Gum Polymers. A series of gum polymers, with properties listed in Table I, were studied using the RPA and Mooney Viscometer. The glass transition temperature (T_g) was determined by differential scanning calorimetry using a TA Instruments Model Q2000 by heating from −120 to 20°C at a heating rate of 10°C/min. The weight average molecular weight (M_w) was determined by Gel Permeation Chromatography using a Waters Alliance 2695 systems with Waters 2410 RI detectors and Tosoh TSKgel GMHxl columns. Polystyrene standards were employed, and Mark–Houwink parameters for each polymer were used to calculate absolute molecular weight using the universal calibration approach.

Filled Compounds. Table II describes several types of rubber compounds, the chain end functionality of the solution (anionic) styrene-butadiene rubber (SBR), the amount and type of particulate filler, and the major polymers. The unit phr is "parts per hundred rubber" which is a weight unit relative to the amount of polymer in the formulation. Some of these formulations were commercial tread formulations for passenger tires and others were experimental formulations used to evaluate new polymer technologies. Typical rubber mixing conditions

Table I. Specifications for Gum Polymers

Gum polymer	T_g (°C)	M_w (g/mol)	Grade/type
Natural rubber (NR)	−65	-	SIR20 Grade
Deproteinized natural rubber (DPNR) (DPNR)	−65	-	From Astlett Rubber (DP-Poly CV)
Synthetic polyisoprene (IR)	-	-	From Goodyear (Natsyn)
Styrene-butadiene rubber (SBR)	−64	260,000	Non-functional; solution SBR
SBR-$SnCl_4$	−30	350,000	One end functional; solution SBR
A-SBR-$SnCl_4$	−42	338,000	Two end functional; solution SBR
Oil extended SBR	−45	294,000	37.5 phr oil; solution SBR
Polybutadiene: Anionic-BR	−96	192,000	Lithium initiator; 40% cis, 10% vinyl
Polybutadiene: Nd-BR	−109	-	Neodymium catalyst; 96% cis, 1% vinyl
Polybutadiene: Ni-BR	−109	252,000	Nickel catalyst; 96% cis, 1% vinyl
Polychloroprene (Neoprene)	-	-	From DuPont (WRT)
Nitrile-Butadiene Rubber (NBR)	-	-	From JSR (N230SV)

were employed using internal mixers. Mixing of Control 1, Expt. 1, and Expt. 2 compounds included one non-productive mixing stage (master batch) and a productive mixing stage (final batch) in an internal mixer. All other compounds were mixed using two non-productive mixing stages and a productive mixing stage in an internal mixer. Sulfur and cure accelerators were added in the productive mixing to allow later vulcanization (crosslinking) of the rubber compounds. The exact details of the compound formulations, mixing conditions, and functional groups on the polymer chains ends are proprietary. Therefore, the functional groups are generically denoted as A, B, C, D, and E. The $SnCl_4$ functionality indicated in Tables I and II is the well-known tin-coupled polymer technology used in anionically polymerized SBR and polybutadiene to promote reactivity with the carbon black surface.[31,32] The SBR microstructure was varied in the series of compounds that included Control 5 and Expts. 9–11, and these polymers were not functionalized. The nanoparticles incorporated to reinforce the rubber compounds were precipitated silica and reinforcing grades of carbon black (CB). The details of the specific particles used are proprietary. Primary particle size (d), aggregate diameter (D), and specific surface area (S) of carbon blacks are well known for the ASTM grades of carbon blacks utilized in the rubber industry.[33] Reinforcing carbon blacks are nanoparticles, and this can be noted, for example, from the characteristics of N110 CB ($d = 17$ nm; $D = 54$ nm; $S = 143$ m^2/g) and N339 CB ($d = 26$ nm; $D = 75$ nm; $S = 96$ m^2/g). Common precipitated silica grades used in passenger tire treads have surface areas in the 170 to 200 m^2/g range, and incorporation of a sulfur-containing silane in silica-filled tread rubber formulations is generally required for commercial viability. The structural features of typical precipitated silica nanoparticles are given by Schaefer et al.[34]

Test Protocols for Mooney Viscometer

For all the samples, the Mooney viscosity was obtained using a MV2000 Mooney Viscometer from Alpha Technologies, equipped with the large rotor. The standard protocol, which meets ASTM D1646, was followed by using a one minute warm up time and a four minute steady shear test at 2 rpm before the Mooney viscosity reading. The large-rotor Mooney value that is the output of this procedure is referred to as ML_{1+4}, and it is a torque result even though it is typically called a viscosity. The units are "Mooney Units" which are related to the instrument torque, and it is quite common to see Mooney viscosities reported without units. For gum polymers, listed in Table I, the test temperature was set at 100°C and for filled rubber compounds, listed in Table II, the test temperature was set at 130°C. The higher temperature for the fully formulated-filled rubber compounds is often employed in the rubber industry so that Mooney viscosity can be measured and the scorch behavior (onset of vulcanization/curing/crosslinking) can be determined at longer times with the use of a single test for both.

Test Protocols for RPA

All measurements were conducted on an Alpha Technologies RPA 2000 rheometer in oscillatory shear mode using a serrated biconical testing geometry with Enterprise Pathfinder software upgraded with Large Amplitude Oscillatory Shear (LAOS) capabilities. A time sweep was performed at a frequency (f) of 0.1Hz (6 cpm) using a constant strain amplitude (γ) for 4 min with data sampling every 30 s, and the torque value at $t = 4$ min was used for comparison with ML_{1+4}. For gum polymers, $\gamma = 7\%$, 10%, 50%, and 100% were tested at 100°C. For filled rubber compounds, $\gamma = 10\%$, 50%, 100%, and 250% were tested at 130°C. A strain amplitude sweep was also performed at 0.1 Hz and 100°C for gum polymers or at 0.1 Hz and 130°C for filled rubber compounds from 0.3% to 250% strain in logarithmic increments. To investigate particle network and flocculation effects, a logarithmic strain sweep from 0.3% to 100% strain was performed at 0.1 Hz and 50°C on the filled compounds, both before curing and after curing. For the latter, the samples were annealed for 15 min at 170°C in the rheometer to vulcanize them before cooling to 50°C to perform the strain sweep. In addition, LAOS testing was performed on the cured and uncured filled rubber compounds at strains of 1%, 3%, 5%, 10%, and 100% at 0.1 Hz and 50°C. The software performs a Fourier transform analysis to quantify the harmonics from the

Table II. Specifications for Rubber Compounds

Rubber compound	SBR functionality[a]	Filler(s)	Polymers
Control 1[b]	none-SBR-none	41phr CB	70phr SBR, 30phr NR
Expt. 1[b]	none-SBR-$SnCl_4$	41phr CB	70phr SBR, 30phr NR
Expt. 2[b]	A-SBR-$SnCl_4$	41phr CB	70phr SBR, 30phr NR
Control 2	none-SBR-none	45phr Silica, 11phr CB	75phr SBR, 25phr NR
Expt. 3	none-SBR-B	45phr Silica, 11phr CB	75phr SBR, 25phr NR
Expt. 4	none-SBR-C	45phr Silica, 11phr CB	75phr SBR, 25phr NR
Control 3	none-SBR-none	55phr Silica, 6phr CB	50phr SBR, 50phr NR
Expt. 5	none-SBR-C	55phr Silica, 6phr CB	50phr SBR, 50phr NR
Expt. 6	D-SBR-D	55phr Silica, 6phr CB	50phr SBR, 50phr NR
Control 4	none-SBR-none	55phr Silica, 6phr CB	50phr SBR, 50phr NR
Expt. 7	none-SBR-E	55phr Silica, 6phr CB	50phr SBR, 50phr NR
Expt. 8	E-SBR-C	55phr Silica, 6phr CB	50phr SBR, 50phr NR
Control 5	none-SBR-none	55phr Silica, 6phr CB	50phr SBR, 50phr NR
Expt. 9	none-SBR-none	55phr Silica, 6phr CB	50phr SBR, 50phr NR
Expt. 10	none-SBR-none	55phr Silica, 6phr CB	50phr SBR, 50phr NR
Expt. 11	none-SBR-none	55phr Silica, 6phr CB	50phr SBR, 50phr NR

[a] Exact chemical details of the polymer functional groups are proprietary and beyond the scope of the article. Therefore, the functional groups are denoted generically as A, B, C, D, and E.
[b] Mixing of Control 1, Expt. 1, and Expt. 2 included one non-productive mixing stage (master batch) and a productive mixing stage (final batch) in an internal mixer. All other compounds were mixed using two non-productive mixing stages and a productive mixing stage in an internal mixer.

stress waveform from the sample response and generates Lissajous plots of stress vs. strain.

RESULTS AND DISCUSSION

Comparison of RPA and Mooney Viscosity Results

In the rubber literature, data correlations have been made by Dick and Pawlowski between the torque values in oscillatory shear mode on the RPA rheometer to the torque values on the steady shear Mooney viscometer for unfilled gum polymer samples.[2,3] Previously, it was found that the complex dynamic viscosity η^* (or complex torque S^*) from RPA at 7% strain, 0.1 Hz, and 100°C correlated well to the final Mooney viscosity values (ML_{1+4}) at 100°C for a wide variety of unfilled elastomers. The present study begins by verifying this correlation for all of the polymers listed in Table I. The results are summarized in Table III for 7% strain, which was previously recommended, as well as 10%, 50%, and 100% strain. Figure 2 shows excellent linear correlations for all of the applied dynamic strain amplitudes. This correlation between steady shear and dynamic viscosities is consistent with the Cox–Merz empiricism for polymer melts.[35,36] The angular frequency (ω) employed for the RPA testing is 0.6 rad/s ($\omega = 2\pi f$; with $f = 0.1$ Hz) compared to the average shear rate in the Mooney viscometer which is in the range from 1.0 to 1.3 s^{-1}.[37,38] These values are in close proximity on a logarithmic scale such that the Mooney viscosity and RPA dynamic torque from this study are expected to be correlated according to the Cox–Merz rule. The lack of influence of dynamic strain amplitude on the statistical strength of the correlation between dynamic torque and Mooney viscosity was anticipated for the gum polymers, because this range of oscillatory strains ($\leq$100%) is lower than the strain value necessary to enter into the nonlinear flow regime of the polymer. Independent strain amplitude sweep tests were performed for several of the polymers (results not reported here) in order to ensure that they behave linearly with applied strain up to 100%. This observed linearity up to $\gamma = 100\%$ is consistent with the large amplitude oscillatory shear studies performed by LeBlanc and de la Chapelle on gum polymers.[26]

While this RPA and Mooney data correlation is verified for unfilled elastomers in this study, the situation is more complex for the particle-filled rubber compounds. It will be shown that exceeding the appropriate strain amplitude (i.e., above the strain range necessary for breakdown of the filler network) is necessary for a correlation to exist between the steady shear Mooney torque and the RPA dynamic torque. The Payne effect is characterized by a steep drop in the elastic modulus with increasing strain amplitude (0.1 to 10%) and the associated increase in loss tangent ($\tan \delta = G''/G'$) which is sometimes called dynamic hysteresis in the rubber industry. This is illustrated in Figure 1. Table II describes several types of rubber compounds, their functionality, the amount and type of filler, and the major polymers. Table IV lists the torque values from several strains (10%, 50%, 100%, 250%) on the RPA and the compound Mooney values at 130°C. Figure 3 shows a linear correlation between RPA and Mooney results only after the filler network has been broken up. Therefore, there is a poor correlation at 10%, contrary to the unfilled polymers, but a good linear correlation at 50%, 100%, and 250%. The strain amplitude test results in Figure 4 at 130°C clearly show that the filler breakup is still occurring at 10% strain but that it has almost completely finished by

Table III. Mooney Viscosity and RPA Results for Gum Polymers at 100°C

Polymer	S^* (dN-m) at 7%	S^* (dN-m) at 10%	S^* (dN-m) at 50%	S^* (dN-m) at 100%	ML_{1+4}
NR	1.40	1.80	8.18	13.57	92.6
DPNR	0.90	1.31	5.65	9.97	57.7
IR	1.02	1.41	5.82	9.95	66.5
SBR	0.70	1.02	4.71	8.15	54.7
SBR-$SnCl_4$	1.32	1.84	8.61	15.35	88.6
A-SBR-$SnCl_4$	1.22	1.76	7.95	13.65	92.7
Oil Ext. SBR	0.64	0.92	4.33	8.04	54.0
Anionic-BR	0.60	0.86	3.90	6.65	40.1
Nd-BR	0.58	0.82	3.83	6.98	40.2
Ni-BR	0.56	0.80	3.74	6.67	45.5
Neoprene	0.59	0.84	3.97	7.08	46.1
NBR	0.36	0.49	2.27	3.88	33.2

50% and 100% strain. The dynamic strain of 250% is near the threshold of the polymer nonlinear flow regime according to our dynamic strain sweeps on selected unfilled elastomers, which agrees with the findings of LeBlanc.[27] Therefore, this strain value would not be ideal to use for the correlation between RPA and Mooney data for filled rubber systems, and the recommendation is therefore $\gamma = 100\%$.

End-Functionalized Polymers and Filler Flocculation

The filler network, which leads to the nonlinear Payne effect, is very complex with regard to its response to applied strain. Understanding the nature of the filler network and minimizing the hysteretic Payne effect are essential to improving the fuel economy of filled rubber compounds used in the treads of automobile tires. The most common approach to reducing the Payne effect is to improve the polymer-filler interactions in the rubber compound. Typically, end functional polymers are synthesized with chemical groups designed to react or interact with the chemical groups on the filler surface during mixing. The chemical reactions and/or associations between the polymer and the filler allow for improved distribution of the filler within the polymer matrix and help to inhibit the formation of filler-filler contacts which contribute to the filler network. As mentioned in the Introduction, the majority of the filler network leading to the Payne effect is formed during annealing of the rubber at higher temperatures, in particular during the cure cycle. The RPA can be used to evaluate the extent of polymer-filler interaction using an approach referred to as the $\delta\Delta G'$ procedure. The $\delta\Delta G'$ at 50°C is calculated for the compounds by subtracting the $\Delta G'$ of a strain amplitude sweep test from $\gamma = 0.3$ to 100% on a rubber sample before cure from the $\Delta G'$ of a similar strain sweep after cure:[15]

$$\delta\Delta G' = \Delta G'_{\text{cured}} - \Delta G'_{\text{uncured}}; \quad (1)$$

where $\Delta G' = G'(\gamma = 0.3\%) - G'\ (\gamma = 100\%)$

The $\Delta G'$ is a parameter to quantify the magnitude of the Payne effect and the related extent of the filler network. The $\delta\Delta G'$ indicates how much of the filler network develops during high temperature annealing, and a lower value indicates better polymer-filler interaction. The "after cure" $\Delta G'$ is much larger in magnitude than the "before cure" value due to filler flocculation, which can occur when the sample is heated to the cure temperature, where the polymer and the filler have more mobility. Figures 5 and 6 show RPA strain sweep results of the Payne effect at 50°C before cure (lower magnitudes of G') and the Payne effect at 50°C after cure (higher magnitudes of G') for the compounds. The results from these strain sweeps are summarized in Table V. When the polymer-filler interaction is strong, there is less ability for filler flocculation to occur and therefore a smaller $\delta\Delta G'$ value is observed. With the single exception of the Expt. 7 compound, the data in Table V show that there is always better polymer-filler interaction when a functionalized polymer is used although some end-modified polymers show more improvement than others. Furthermore, the results demonstrate that it is not necessarily advantageous to have a two-end functional polymer as can be noted from

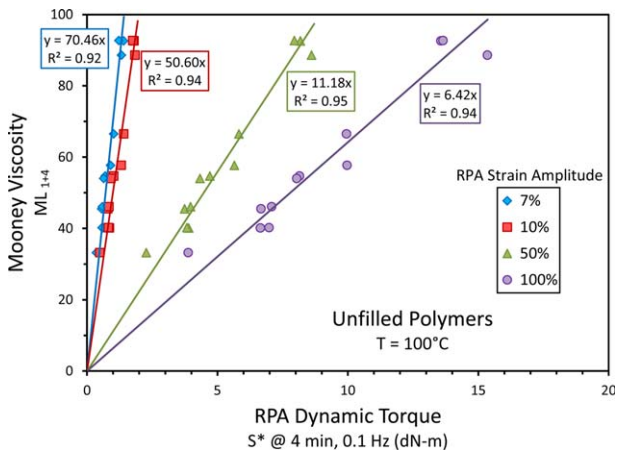

Figure 2. Comparison of steady shear Mooney Viscosity with RPA dynamic torque for gum polymers at 100°C at the indicated strain amplitudes. The *y*-intercept was fixed at zero for the linear fits to the data. [Color figure can be viewed in the online issue, which is available at wileyonlinelibrary.com.]

Table IV. Mooney Viscosity and RPA Results for Rubber Compounds at 130°C

Compound	S* (dN-m) at 10%	S* (dN-m) at 50%	S* (dN-m) at 100%	S* (dN-m) at 250%	ML_{1+4}
Control 1	1.27	3.17	5.05	10.34	43.2
Expt. 1	1.42	4.04	6.38	11.85	46.6
Expt. 2	2.34	6.89	10.18	16.49	68.0
Control 2	1.48	2.66	3.78	6.53	28.9
Expt. 3	1.69	4.48	6.33	9.92	44.8
Expt. 4	2.64	6.15	8.40	12.86	58.1
Control 3	3.26	5.04	6.42	10.00	46.5
Expt. 5	3.80	8.03	10.50	14.85	71.9
Expt. 6	4.29	9.51	12.48	17.57	86.0
Control 4	3.50	4.93	6.38	10.80	50.5
Expt. 7	3.25	5.01	6.55	11.18	49.8
Expt. 8	3.94	7.78	10.56	14.62	68.5
Control 5	2.85	4.58	6.08	10.29	47.6
Expt. 9	2.48	4.31	5.67	9.56	42.7
Expt. 10	3.12	5.06	6.82	11.64	52.4
Expt. 11	2.97	4.64	5.99	9.68	43.6

comparing the $\delta\Delta G'$ data for compounds Expts. 5 and 6 in Table V. More influential is the nature of the functional group and its ability to react with the filler surface and prevent filler flocculation rather than the quantity of the functional groups.

Fourier Transform Rheometry and Linear-Nonlinear Dichotomy

This study has illustrated: (1) the linear viscoelastic response in unfilled gum polymers up to 100% applied strain, which allows for a good correlation between oscillatory shear and steady shear results at all of the strain amplitudes investigated; and (2) the nonlinear response of the filler network (Payne effect) in particle-reinforced rubber compounds at very low strain amplitudes (<10%) that necessitates the use of higher dynamic strains (ca. 100%) for good correlation between the RPA torque and Mooney torque. The complexity of the filled rubber compounds is termed a "linear-nonlinear dichotomy"[11] based on the unusual coexistence of linear and nonlinear viscoelastic characteristics as was mentioned in the Introduction. Fourier transform rheometry is a critical tool for further investigating this behavior. It is applied to the recorded raw signals from the rheometer for the time-dependent strain input and torque output to resolve the waveforms and harmonics, with the odd being the most significant (i.e., 1st, 3rd, 5th).

The RPA utilized in this study is integrated with software to conduct Fourier transform rheology analyses. For a strain-

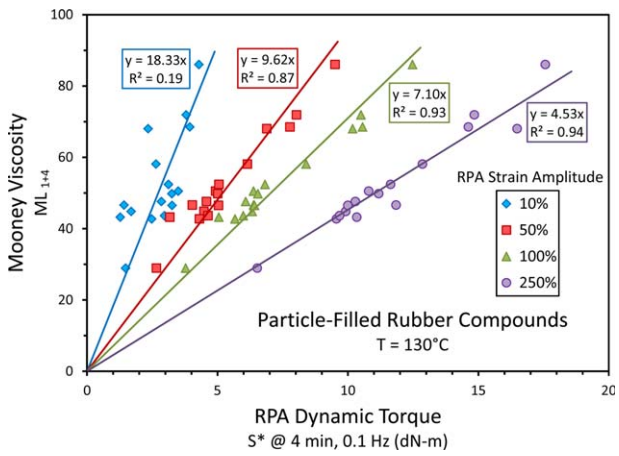

Figure 3. Comparison of steady shear Mooney Viscosity with RPA dynamic torque for particle-filled rubber compounds at 130°C at the indicated strain amplitudes. The *y*-intercept was fixed at zero for the linear fits to the data. [Color figure can be viewed in the online issue, which is available at wileyonlinelibrary.com.]

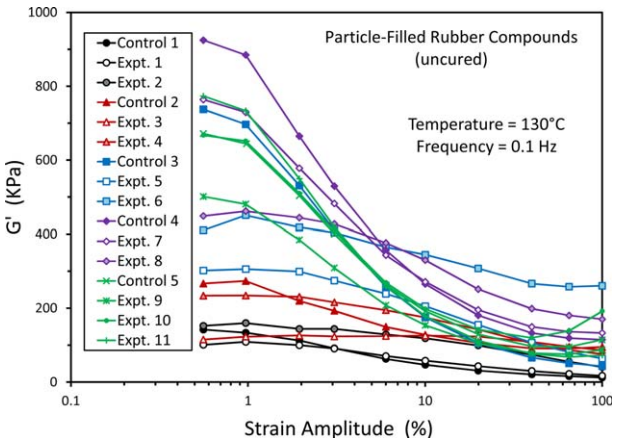

Figure 4. Storage modulus versus strain amplitude from RPA strain sweep at 130°C and 0.1 Hz for the indicated filled rubber compounds. [Color figure can be viewed in the online issue, which is available at wileyonlinelibrary.com.]

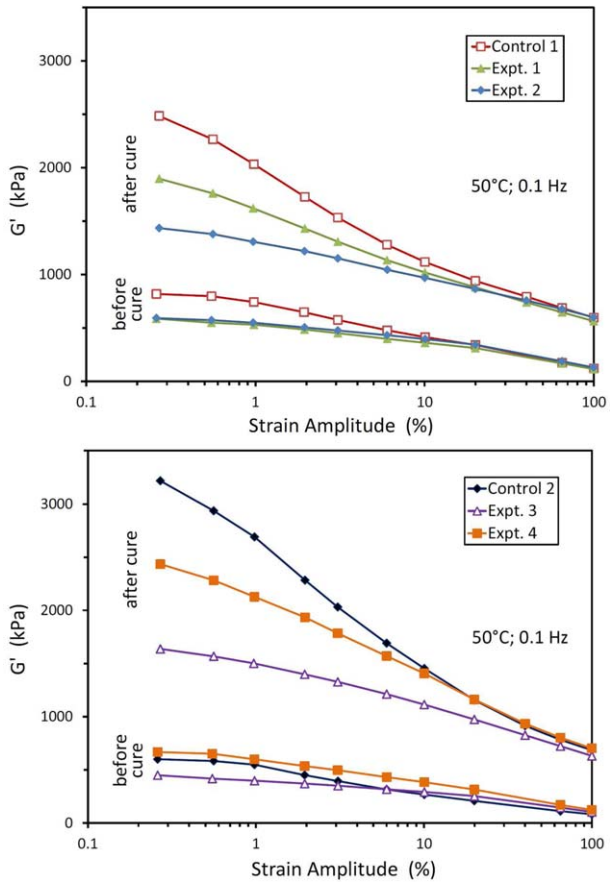

Figure 5. Strain sweep results from RPA at 50°C and 0.1 Hz comparing the before cure Payne effect (lower G' magnitudes) and after cure Payne effect (higher G' magnitudes) for the indicated rubber compounds. [Color figure can be viewed in the online issue, which is available at wileyonlinelibrary.com.]

controlled rheometer like the RPA, the oscillatory strain input that is applied to the sample is:

$$\gamma(t)=\gamma_0 \sin(\omega t) \tag{2}$$

where γ_0 is the strain amplitude which is sometimes called the dynamic strain and is frequently represented without the 0 subscript. The nonlinear stress response can be represented by a Fourier series:[39]

$$\sigma(t;\ \omega,\gamma_0)=\gamma_0 \sum_{n\ \text{odd}} \{G'_n(\omega,\gamma_0)\sin(n\omega t)+G''_n\ (\omega,\gamma_0)\cos(n\omega t)\} \tag{3}$$

Only odd harmonics are considered to be significant because the response of a material should not change if the coordinate system is reversed. If the stress output is sinusoidal in shape and simply offset from the time-dependent strain input, then the material is linear viscoelastic and can be simply characterized through the use of only the first-harmonic coefficients, G'_1 and G''_1. These are the common output of commercial rheometers, G' and G'', but these parameters are only meaningful when the material is linear viscoelastic in the sense that the stress output is sinusoidal in shape and simply offset from the oscillatory strain input. The detection of significant higher order harmonics (3rd, 5th, etc.) using Fourier transform rheometry indicates nonlinear viscoelastic behavior for a material, and the shape of the stress output is distorted relative to a sine wave.

Fourier transform rheometry studies were performed on the RPA for three filled rubber compounds in the uncured and cured states. The compounds tested were Control 1, Expt. 1, and Expt. 2. Only the results for the Expt. 2 rubber compound are shown. However, the Control 1 and Expt. 1 materials performed in the same general manner. Lissajous plots of stress versus strain can also be generated from the dynamic viscoelastic testing with the RPA, with symmetrical behavior around the major axis of an elliptical response indicating linear viscoelastic behavior.[30] The waveforms and Lissajous plots are shown in Figures 7–9 for the Expt. 2 material. These results show very good linearity in the viscoelastic response at the strains (1%–10%) that are in the middle of the strongly "nonlinear" Payne effect region. Linear viscoelastic behavior is maintained at each strain in the range where the filler network goes through a significant structural breakdown/rearrangement. There is some small sign of nonlinearity beginning in the sample at 100% applied strain as shown in the insets of Figures 8 and 9 for

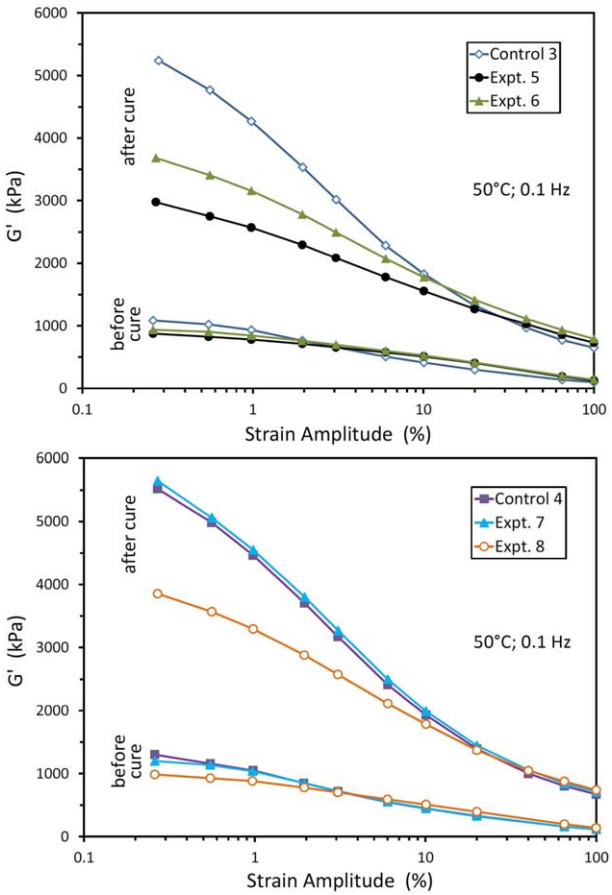

Figure 6. Strain sweep results from RPA at 50°C and 0.1 Hz comparing the before cure Payne effect (lower G' magnitudes) and after cure Payne effect (higher G' magnitudes) for the indicated rubber compounds. Note the different scaling for the y-axis in comparison to Figure 5. [Color figure can be viewed in the online issue, which is available at wileyonlinelibrary.com.]

Table V. RPA Results for Filler Flocculation

RPA: Between 0.3% and 100% strain; 50°C; 0.1 Hz			
Compound	Uncured $\Delta G'$ (kPa)	Cured $\Delta G'$ (kPa)	$\delta\Delta G'$ (kPa)
Control 1	698	1889	1191
Expt. 1	472	1333	861
Expt. 2	462	835	373
Control 2	518	2535	2017
Expt. 3	346	1007	661
Expt. 4	545	1732	1187
Control 3	986	4590	3604
Expt. 5	749	2245	1496
Expt. 6	795	2890	2095
Control 4	1187	4847	3660
Expt. 7	1086	4931	3845
Expt. 8	846	3116	2270

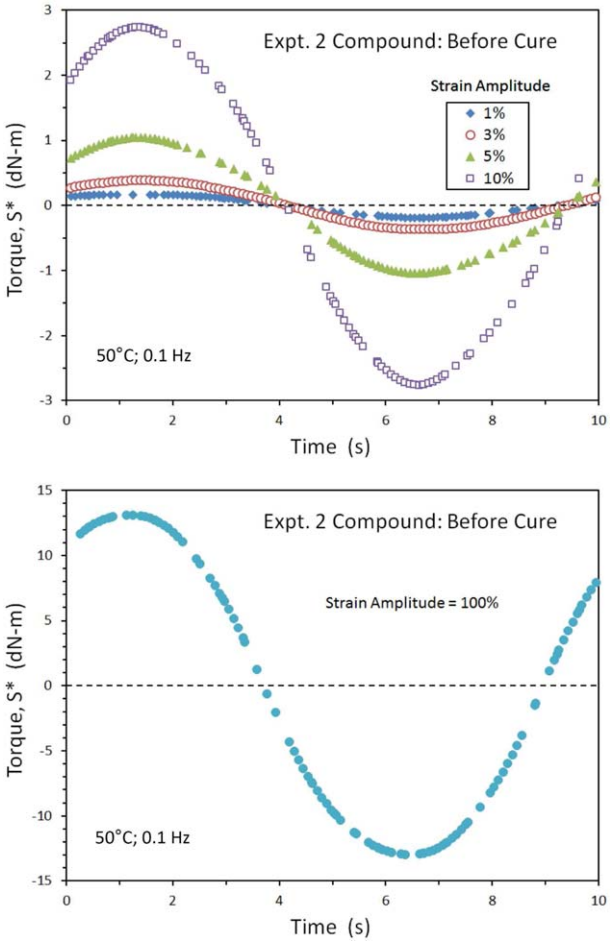

Figure 7. LAOS waveforms at 50°C and 0.1 Hz for various applied strains on the RPA for the uncured Expt. 2 rubber compound. The responses are *nonlinear* based on the decrease in dynamic modulus with strain amplitude, but yet they are also *linear* at each strain based on the simple sinusoidal shape of the time-dependent stress. [Color figure can be viewed in the online issue, which is available at wileyonlinelibrary.com.]

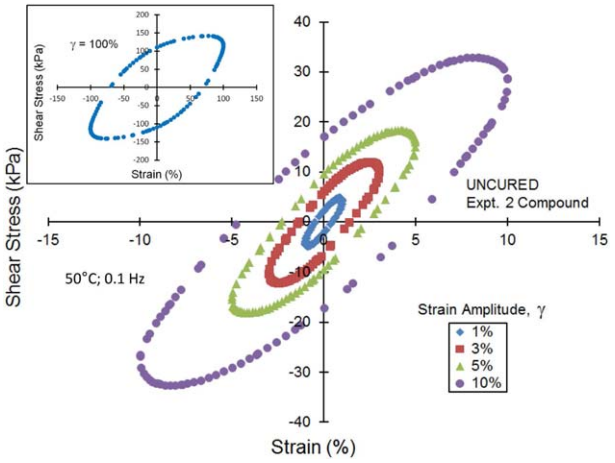

Figure 8. LAOS Lissajous Plot of Shear Stress (kPa) versus Strain (%) on RPA for the uncured Expt. 2 rubber compound at 50°C and 0.1 Hz. Inset is the Lissajous Plot for 100% strain. [Color figure can be viewed in the online issue, which is available at wileyonlinelibrary.com.]

uncured and cured samples, respectively. However, Figures 10 and 11 show that the 3rd and 5th harmonics are essentially negligible compared to the 1st at all of the strain amplitudes, including $\gamma = 100\%$.

There are two important consequences of the observed linear-nonlinear dichotomy of particle-filled elastomers, one applications-related and one fundamental. From an applied standpoint, the fact that the stress response of these filled polymer systems to oscillatory strain is simply sinusoidal in shape, even though the dynamic storage and loss moduli depend strongly on strain amplitude, indicates that the G' and G'' values determined from the strain sweeps are meaningful characteristics of the particle-filled materials at each strain in the range up to approximately 100% strain. This was observed for the commercially important filled rubber compounds included in this study, in both the cured (vulcanized) and uncured states.

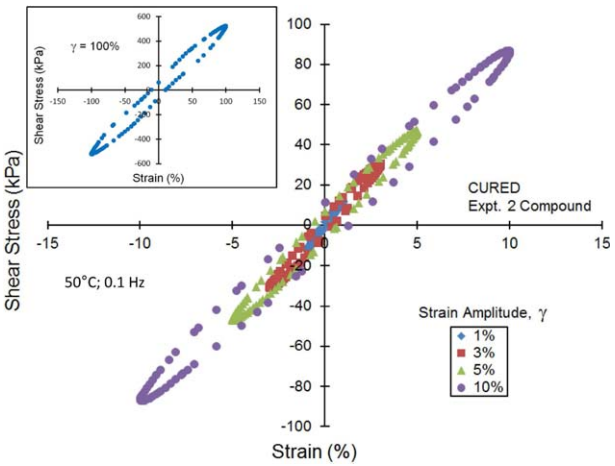

Figure 9. LAOS Lissajous Plot of Shear Stress (kPa) versus Strain (%) on RPA for the cured Expt. 2 rubber compound. Inset is the Lissajous Plot for 100% strain. [Color figure can be viewed in the online issue, which is available at wileyonlinelibrary.com.]

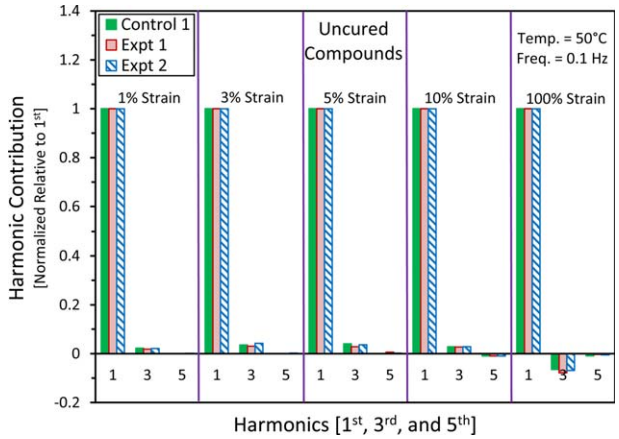

Figure 10. 1st, 3rd, and 5th Harmonics from the Fourier Transform of the LAOS results from Control 1, Expts. 1, and 2 rubber compounds in the uncured state. [Color figure can be viewed in the online issue, which is available at wileyonlinelibrary.com.]

This is not the case in traditional nonlinear behavior of polymers where a change in the dynamic moduli with γ is generally accompanied by distortion of the time-dependent stress response relative to a simple sine waveform. For unfilled polymers at temperatures well above T_g, such as the elastomers studied in this investigation, this nonlinear viscoelastic behavior usually occurs at high strains (>100%) compared to the strain range (0.1% to 10%) associated with the Payne effect type of nonlinearity that occurs when such polymers contain sufficient loading of particles. Concerning the fundamental implications of the linear-nonlinear dichotomy, this behavior further highlights the heterogeneous nature of the filler network that was revealed previously by dynamic strain hole burning experiments ("mechanical aging") at two sequential strain amplitudes.[40] The findings here also support the notion that the reformation process for particle-particle contacts is slow while strain oscillation is proceeding. In other words, once the parts of the filler network that are sensitive to the particular dynamic displacement are broken in the first few strain cycles, they do not reform during the subsequent cycles from which the viscoelastic properties are measured. The material is softened as the strain amplitude is increased and the reinforcing filler network is progressively disrupted, but yet linear viscoelastic behavior is maintained at each strain.

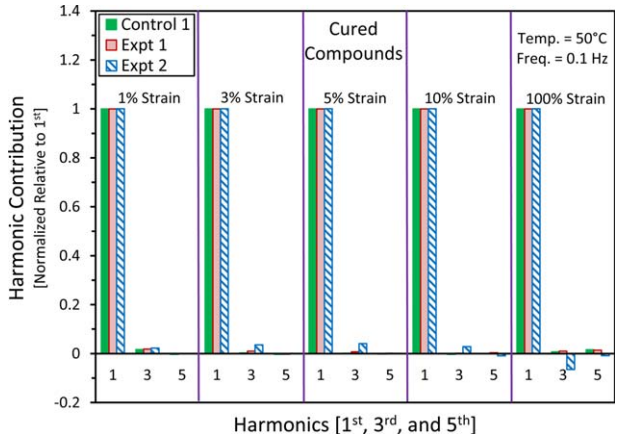

Figure 11. 1st, 3rd, and 5th Harmonics from the Fourier Transform of the LAOS results from Control 1, Expts. 1, and 2 rubber compounds in the cured state. [Color figure can be viewed in the online issue, which is available at wileyonlinelibrary.com.]

It must be noted that the first few cycles, during measurement at the specified set of conditions in a dynamic test, are not used for analyzing viscoelastic properties in standard testing protocols using commercial dynamic mechanical analyzers or rheometers in oscillatory mode. It is expected that the rich physics related to the filler network break-up and reformation can be further revealed by studying these transitions from rest or between different strain amplitudes.

CONCLUSIONS

The tire industry spans the decades as a field requiring both practical testing of viscoelasticity and processability as well as a fundamental, mechanistic understanding of the underlying rubber physics. The practical processing side of this study correlated the Mooney viscosity at 130°C for filled rubber compounds to the complex dynamic torque on the RPA rheometer at test conditions of 130°C, 100% strain, and 0.1 Hz. This differs significantly from the observations for unfilled gum polymers wherein correlations were evident at much lower strain amplitudes. In filled rubber compounds, the filler network plays an important role in the flow properties such that the applied strain amplitude must exceed the Payne effect region (0.1% to 10%) before a correlation can exist between the steady shear Mooney viscosity and the oscillatory shear viscosity. It is the linear-nonlinear dichotomy of the Payne effect which is the focus of the fundamental component of this investigation. The use of Fourier transform rheometry showed that the response of filled rubber compounds, both cured and uncured, to forced oscillation remained sinusoidal, absent any higher order harmonics, even though the dynamic moduli were so strongly influenced by the strain amplitude. It was also demonstrated that increasing the polymer-filler interactions by using end-functionalized polymers inhibited the filler flocculation process, resulting in less extensive filler networking (reduced magnitude of the Payne effect) as shown from the strain-dependence of the dynamic storage modulus.

ACKNOWLEDGMENTS

Bridgestone Corporation is acknowledged for approving the publication of this work. The testing contributions of Mark McEwen and Jon Misner are greatly appreciated.

REFERENCES

1. ASTM Standard D1646-07, Standard Test Methods for Rubber-Viscosity, Stress Relaxation, and Pre-Vulcanization Characteristics (Mooney Viscometer), 09.01, 1991.
2. Pawlowski, H.; Dick, J. *Rubber World* **1992**, *206*, 35.
3. Pawlowski, H.; Dick, J. *Rubber World* **1995**, *211*, 20.
4. Mark, J. E.; Erman, B.; Eirich, F. R., Eds. Science and Technology of Rubber, 3rd ed.; Elsevier: London, **2005**.

5. Payne, A. R. *J. Appl. Polym. Sci.* **1962**, *6*, 57.
6. Roland, C. M. *J. Rheol.* **1990**, *34*, 25.
7. Robertson, C. G.; Wang, X. *Phys. Rev. Lett.* **2005**, *95*, 075703.
8. Robertson, C. G.; Bogoslovov, R.; Roland, C. M. *Phys. Rev. E* **2007**, *75*, 051403.
9. Wang, M.-J. *Rubber Chem. Technol.* **1999**, *72*, 430.
10. Heinrich, G.; Klüppel, M. *Adv. Polym. Sci.* **2002**, *160*, 1.
11. Robertson, C. G.; Wang, X. *Europhys. Lett.* **2006**, *76*, 278.
12. Chazeau, L.; Brown, J. D.; Yanyo, L. C.; Sternstein, S. S. *Polym. Compos.* **2000**, *21*, 202.
13. Hall, D. E.; Moreland, J. C. *Rubber Chem. Technol.* **2001**, *74*, 525.
14. Schuring, D. J.; Futamura, S. *Rubber Chem. Technol.* **1990**, *63*, 315.
15. Lin, C. J.; Hergenrother, W. L.; Alexanian, E.; Böhm, G. G. A. *Rubber Chem. Technol.* **2002**, *75*, 865.
16. Bohm, G. A; Tomaszewski, W.; Cole, W.; Hogan, T. *Polymer* **2010**, *51*, 2057.
17. Scurati, A.; Lin, C. J. *Rubber Chem. Technol.* **2006**, *79*, 170.
18. Böhm, G. G. A; Nguyen, M. N. *J. Appl. Polym. Sci.* **1995**, *55*, 1041.
19. Schwartz, G. A.; Cerveny, S.; Marzocca, A. J.; Gerspacher, M. Nikiel, L. *Polymer* **2003**, *44*, 7229.
20. Meier, J. G.; Klüppel, M. *Macromol. Mater. Eng.* **2008**, *293*, 12.
21. Robertson, C. G.; Lin, C. J.; Bogoslovov, R. B.; Rackaitis, M.; Sadhukhan, P.; Quinn, J. D.; Roland, C. M. *Rubber Chem. Technol.* **2011**, *84*, 507.
22. Mihara, S.; Datta, R. N.; Noordermeer, J. W. M. *Rubber Chem. Technol.* **2009**, *82*, 524.
23. Lin, C. J.; Hogan, T. E.; Hergenrother, W. L. *Rubber Chem. Technol.* **2004**, *77*, 90.
24. Scurati, A.; Lin, C. J. *Rubber Chem. Technol.* **2006**, *79*, 170.
25. Pan, X.-D.; Yan, Y. Y.; Qin, Z.; Brumbaugh, D. R.; Sadhukhan, P. *Rubber Chem. Technol.* **2012**, *85*, 526.
26. Leblanc, J. L.; de la Chapelle, C. *Rubber Chem. Technol.* **2003**, *76*, 979.
27. Leblanc, J. L. *Rubber Chem. Technol.* **2005**, *78*, 54.
28. Leblanc, J. L. *J. Appl. Polym. Sci.* **2006**, *100*, 5102.
29. Leblanc, J. L. *J. Appl. Polym. Sci.* **2005**, *95*, 90.
30. Ewolt, R. H.; Hosoi, A. E.; McKinley, G. H. *J. Rheol.* **2008**, *52*, 1427.
31. Tsutsumi, F.; Sakakibara, M.; Oshima, N. *Rubber Chem. Technol.* **1990**, *63*, 8.
32. Ulmer, J. D.; Hergenrother, W. L.; Lawson, D. F. *Rubber Chem. Technol.* **2004**, *77*, 90.
33. Hess, W. M.; McDonald, G. C. *Rubber Chem. Technol.* **1983**, *56*, 892.
34. Schaefer, D. W.; Suryawanshi, C.; Pakdel, P.; Ilavsky, J.; Jemian, P. R. *Physica A* **2002**, *314*, 686.
35. Cox, W. P.; Merz, E. H. *J. Polym. Sci.* **1958**, *28*, 619.
36. Mead, D. W. *Rheol. Acta.* **2011**, *50*, 837.
37. Dick, J. S. Basic Rubber Testing: Selecting Methods for a Rubber Test Program; ASTM International: Bridgeport, NJ, **2003**; p 22.
38. Brown, R. P. Physical Testing of Rubber, 2nd ed.; Elsevier Applied Science Publishers: London, **1986**; p 93.
39. Dealy, J. M.; Wissbrun, K. F. Melt Rheology and Its Role in Plastics Processing: Theory and Applications; Van Nostrand Reinhold: New York, **1990**.
40. Wang, X.; Robertson, C. G. *Europhys. Lett.* **2007**, *79*, 18001.